24

Rock Fracture Image Segmentation Algorithms

Weixing Wang
School of Information Engineering, Chang'an University, Xi'an China

1. Introduction

Since rock fracture is a key property for different rock engineering applications, rock fracture measurement is often carried out in classifying the rock mass. Most geo-mechanics models (e.g. finite element) are of the equivalent continuum type in which fractures are represented not individually, but by their influence on a large element of the rock mass. Elastic modulus, for example, is obtained either by large-scale testing of rock containing many joints, or, at less expense, by applying a reduction factor to the modulus obtained from small-scale tests on intact rock. Other models (e.g. those based on the key block concept) are capable of taking into account the position and mechanical characteristics of individual fracture. The shear strength of a fracture can be estimated from its roughness together with strength and thickness of filling materials, using a variety of empirical or semi-empirical methods. The techniques of image processing and segmentation can be applied as a power tool for obtaining more detailed information and analysis of rock fractures.

In this chapter, we firstly to give an overview of the current status of the rock fracture processing research, then, give a brief description of visual rock fracture properties and classify the types of rock fractures, finally, we summarize the work we have done in last year.

1.1 Overview of image processing literature on rock fractures

A series of the previous research work is related to the program for storage of high level radioactive waste. A repository represents changes of numerical, thermal, hydraulic and chemical conditions, which are studied by using numerical models. The models are based on the geological conditions of the site, especially characteristics of the fracture network and properties of single fracture, since these parameters control the flow through the rock mass.

Let us now turn to image processing and measurements of rock fractures/ 1-24/ . Maria Johansson (1999) in her Lic. Thesis, presented three different algorithms for single rock fracture or crack detection. Quanhong Feng (1996) in his master thesis presented the BIP system for acquiring borehole images, and studied the measurement of the orientation of a single joint in a borehole, and other fracture properties. Masahiro Iwano (1995) in his doctoral thesis reviewed the research history of hydro-mechanical characteristics of a single rock joint, and studied a series of lab test and theatrical analysis. For the single joint measurement by using image technique, Eva Hakami (1995) in her doctoral thesis presented a method to measure aperture and roughness, and analyzed the relationship between aperture (and roughness) and hydro-mechanical characteristics.

For multiple fractures on an image, Reid and Harrison (2000) presented a semi-auto tracing method for rock fractures. Lemy and Hadjigeorgiou (2003) developed a auto-tracing method for rock fractures based on edge detection and neural network. Parviz Soroushian (2003) proposed an algorithm for fracture image binarization on theirlaboratory SEM images. Similar work have been done by John Kemeny, Randy Post, 2003, Wang, W.X. & Stephansson, O., 1997, Lee SW, Kim YJ. , 1995, Wang L, Pavlidis T., 1993, Harrison JP, 1993, G. X. Sun, D. J. Reddish and B. N. Whittaker, 1992, Hu J, Sakoda B, Pavlidis T., 1992, Whittaker RN, Singh RN, Sun G., 1992, Finn Ouchterlony, 1990, Tanimoto C, Murai S, Kiyama Joshi AK.,1989, John A. Franklin, Norberth H. Maerz and Caralyn P. Bennett, 1988. For the three-dimensional estimation, the previous work has been done by John Kemeny, Randy Post, 2003, Zou Dingxiang, Weixing Wang and Ma Bailing, 1986. Lyman (2003) has used neural network technique to detect fractures.

In the well-known BIPS system, rock fractures (curves) are traced based on input points (the more points, the more accurate is the tracing), to fit curves on theoretical sinusoidal shape (distribution). It is not an image processing or matching algorithm, the color or grey information is not needed.

In order to make measurements of rock fractures (or spacing, discontinuities) easy and sufficiently for the accurate analysis of rock mechanics and engineering geology, we combined all the knowledge we have, to establish a programming library for rock fracture measurement and analysis, and developed several rock fracture measurement algorithms on the rock mechanics and geology applications. Now I have setup an algorithm library, which includes a number of algorithms for rock fracture analysis and classification.

1.2 Visual rock fracture properties and classification for image segmentation

In most cases, rock surface is rough, except for the variations of colors and gray- scales, three dimensional surface roughness is the another property comparing to other applications. For image processing and analysis, fractures or cracks belong to linear curved objects; the length of an object is much longer than width. Inside the object, it may be empty or filled by different materials. The filling materials are with different colors. Since the large width and color variation, it is usual that there are many gaps on one object. Another property is that some fault object appears on an image due to rough and noised surface. Random and multiple fractures may form a complicated network where fractures cross each other. All the properties make image processing and segmentation harder than other applications. The following are reprehensive examples for different types of fractures or cracks.

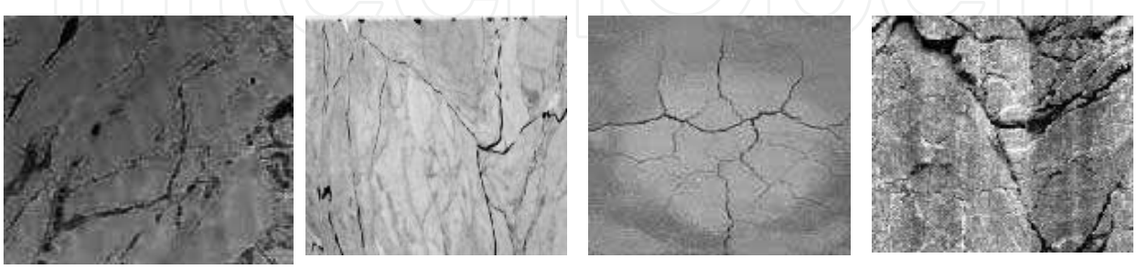

(a) (b) (c) (d)

Fig. 1. Four different types of rock fractures: (a) fractures are not continuous, (b) fractures have different gray-scales, (c) fractures form a network, and (d) very rough surface.

1.3 Summary of our work

In image processing, as a normal work sequence, we first used global filters and local filters to remove the noise and make gray variation correction, which is called image preprocessing. After image preprocessing, the image quality is increased, the remaining work is to abstract rock fractures from background, so-called image segmentation. In image segmentation part, we compared and used thresholding algorithms to binarize the rock fracture images for a rough analysis, in addition to this, both edge based algorithms and region similarity algorithms are tested and studied. Since the edge based algorithm can detect fracture boundary location accurately, and region similarity algorithms are better to alleviate producing extra noise, however, which type of algorithms, is selected to use, depending on the image properties. In the study, we found that the combination (or fusion) of the two or three types of image segmentation algorithms is a best way for segment our rock fracture images, but we have not fully used this procedure (it is still under development) yet in this work period. Since our image is resin injection fracture image, the simplest algorithm is image binarization, therefore we tested five different auto-thresholding algorithms which are widely used in the world. As the comparing result, we selected two binarization algorithms for our images; the one is Optimal binarization algorithm, and the other is Between class variance binarization algorithms. In edge based segmentation algorithm study, we tested popularly used edge detectors such as Canny edge detector and Robert edge detector etc. We found out that week and thin fractures cannot be detected y using these algorithms, since fractures are ridge objects, as an alternative, we developed a new edge detection algorithm for these kinds of edges. For high resolution images, the fractures are relatively thick: on the surface, a lot of white noise appears. To overcome this problem, we tried multi-scale technique for both region similarity and edge based algorithms. In conclusion, we tested 10 different preprocessing algorithms, five image binarization algorithms, and five edge detection algorithms. We developed and modified five different algorithms for image enhancement and segmentation. For our rock fracture images, we mainly used the modified image binarization algorithms.

2. Image preprocessing

The aim of image preprocessing is to enhance images for better visualization and processing. Image preprocessing techniques can be classified into global operators and local operators/ 25/ . Linear contrast stretch and histogram equalization are two of the most widely used global operators. Adaptive histogram-equalization, contrast-limited adaptive histogram equalization, kernel filters, morphological functions and multi-scale enhancement belong to the local operators. While the global methods use a transformation applied to all the pixels of the image, the later methods use input-output transformation that varies adaptively with the local characteristics of the image. The typical types of image preprocessing can be expressed as:

Global operators: $f_{new}(x,y) = Trans\left(f_{original}(x,y)\right)$

Local operators: $f_{new}(x,y) = f_{original}(x,y) - Filter(x,y) + Const.$

Image enhancement algorithms have been designed to process a given image so the results are better than the original image for their applications or objectives. When the objective is to improve perceptual aspects, desirable image preprocessing can be performed by the contrast and dynamic range modification.

In this study, to enhance the fracture image for further processing and segmentation, we tried the both methods. To make comprehensively understanding the testing methods, we, first, briefly introduce some basic idea of digital images in separated sub-sections.

2.1 Image converting from color to gray scale

Notation: image converting from color to gray scale:

A grey scale image: $f(x,y)$ has $L(i=1,2,..,l \le 256)$ gray levels for each of image pixels, x, y are image sizes in horizontal and vertical directions respectively.

A color image (RGB) is a combination of three images: $F\{f_r(x,y), f_g(x,y), f_b(x,y)\}$.

If one converts a color image to a grey scale image, an general converting equation can be presented as:

$$F \Rightarrow f(x,y) = \alpha \cdot f_r(x,y) + \beta \cdot f_g(x,y) + \gamma \cdot f_b(x,y) \ , (\alpha + \beta + \gamma = 1)$$

As an example in Fig. 2, we split a color image into R.G..B three images, the three images are different (the worst one may be the blue image), the differentiation is image dependent. In the Fig.3, the color image is split into R.G. $(\alpha + \beta + \gamma = 0.5 + 0.5 + 0.0 = 1)$, R.B.

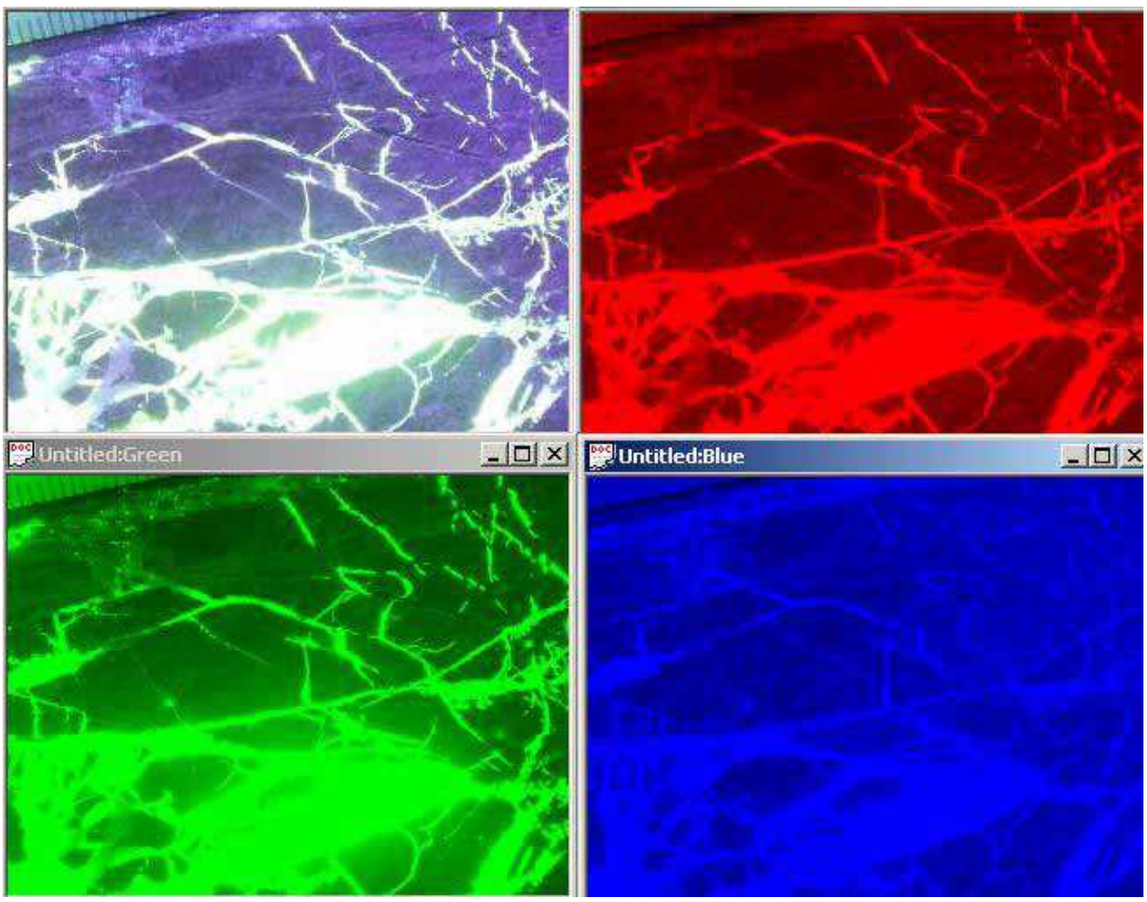

Fig. 2. A color fracture image is split into R.G..B. three images

($\alpha+\beta+\gamma=0.5+0.0+0.5=1$), and G.B ($\alpha+\beta+\gamma=0.0+0.5+0.5=1$) images. The each of the new images is a combination of two channel images, which make some new presentations for the original image. In the example, the yellow image may show fracture clearer than others.

Except for R.G..B, a color pixel can also be divided into the three values of intensity (I), hue (H) and saturation (S), which is another way to represent a color image. An example is shown in Fig. 4. For fractures, the best image may be the combination of light intensity (I) and color hue (H).

When a color image is to be converted to a gray scale image, the new image pixel value can also be calculated based on the R.G..B values or I.H.S. values in different ways. Fig. 5 shows that the above color image is converted to a gray scale image by using minimum or maximum R.G..B.values, which means that for each of the image pixels, checking its R.G..B. values, and choosing the minimum or maximum value of the three values, as input for the new image. In our application image, it is obviously that the minimum converting is better.

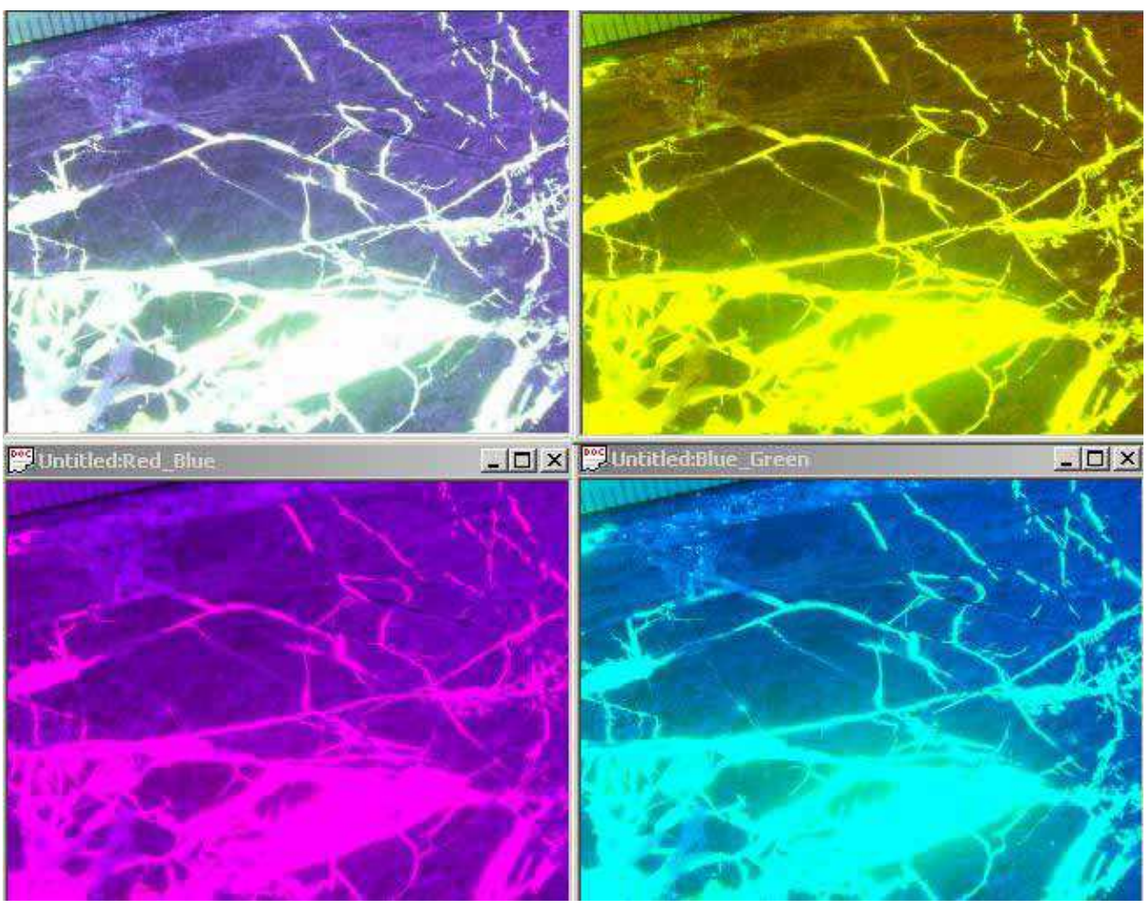

Fig. 3. A color fracture image is split into RG..RB.GB. three images.

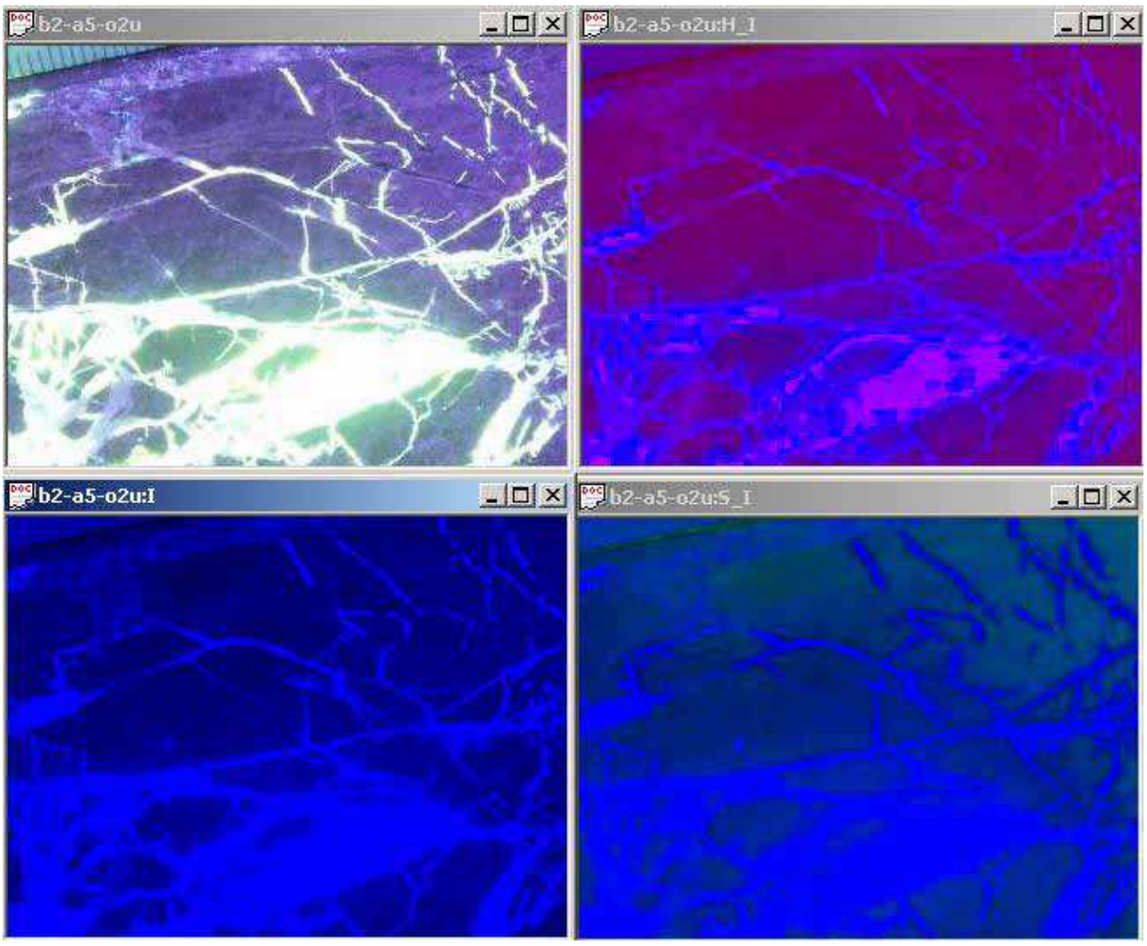

Fig. 4. A color fracture image is split into HI, I and SI three images

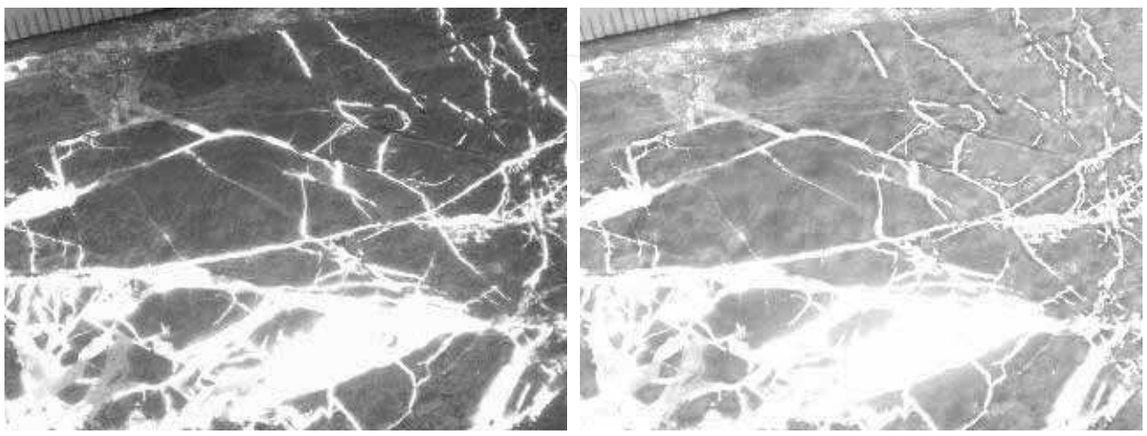

Fig. 5. The color fracture image is converted into a gray image. (a) Converted by using minimum R.G..B.values, and (b) Converted by using maximum R.G..B.values.

Anyhow, a color image includes a lot of information, some information is useful, and some cannot be used, which depends on the requirements for image processing and analysis. All the image converting methods belong to global operators. In our study, since we only consider the gray scale image segmentation, we have not used the color information yet, we normally directly convert a color image by using Minimum or Middle operators, in a few cases, and we also used the combination of GB image to obtain a gray scale image. To fully use the available color information, we may need more tests and studies.

2.2 Comparison of image preprocessing operators

No matter a color image or a gray scale image, a number of image preprocessing operators can be used for image enhancement. For a gray scale image, an operator acts on one image, and for a color image, an operator acts on three images (R.G.B.) respectively. Based on our rock fracture characteristics, we tested several widely used operators on the images. Based on our utilities, we classify all the tested operators into two types: the one is for image noise removal, and the other is for rock fracture sharpening on images.

In Fig. 6, we compared five different operators for a color rock fracture image. In Fig. 6(b), the operator is a 3x3 kernel with a Median filter operation (local operator) on the image, on the new image, the noise points and lines are removed, but the image is blurred; (c) Morphological operation (local operator): simple opening and closing, the operation result is similar to the median filter, it maybe more better for removing noise lines or curves; (d) Linear stretch (global operator): stretching the range of gray scales, it make intensity contrast more better.; (e) Sharpening (local operator): make fracture more shaper, but noise arising; and (f) Exponent transformation (global operator): decrease the gray values of the non-fracture regions.

For our images, we often used the operators of Exponent transformation, Linear stretch and Median filters. Since this is a testing stage, we have no an automatic procedure for enhancement of the rock fracture images currently, we may need to develop that in the next step of work. The auto-procedure development will be based on the further processing-image segmentation (fracture delineation or tracing) requirements.

3. Fracture delineation or tracing

After image preprocessing, the next is image segmentation-fracture tracing. The image segmentation is an old and topic subject of image analysis and pattern recognition. The current tendency is to combine different image segmentation algorithms for special application domain/ . Our domain is rock fractures or fracture network.

3.1 Image thretholding

The scope of the present part is thresholding algorithms applied to a specific DOMAIN, that of rock fractures, in rock engineering. Fractures can be natural or man-made, where the former is of substantial interest in rock engineering applications. We stresses that the study deals with thresholding applied to a special domain rather than thresholding in general, because (a) the general problem is rather unspecified, (b) there is a greater chance of evaluating thresholding algorithms, if limiting the domain of possible images, and (c) there is the application of interest to us.

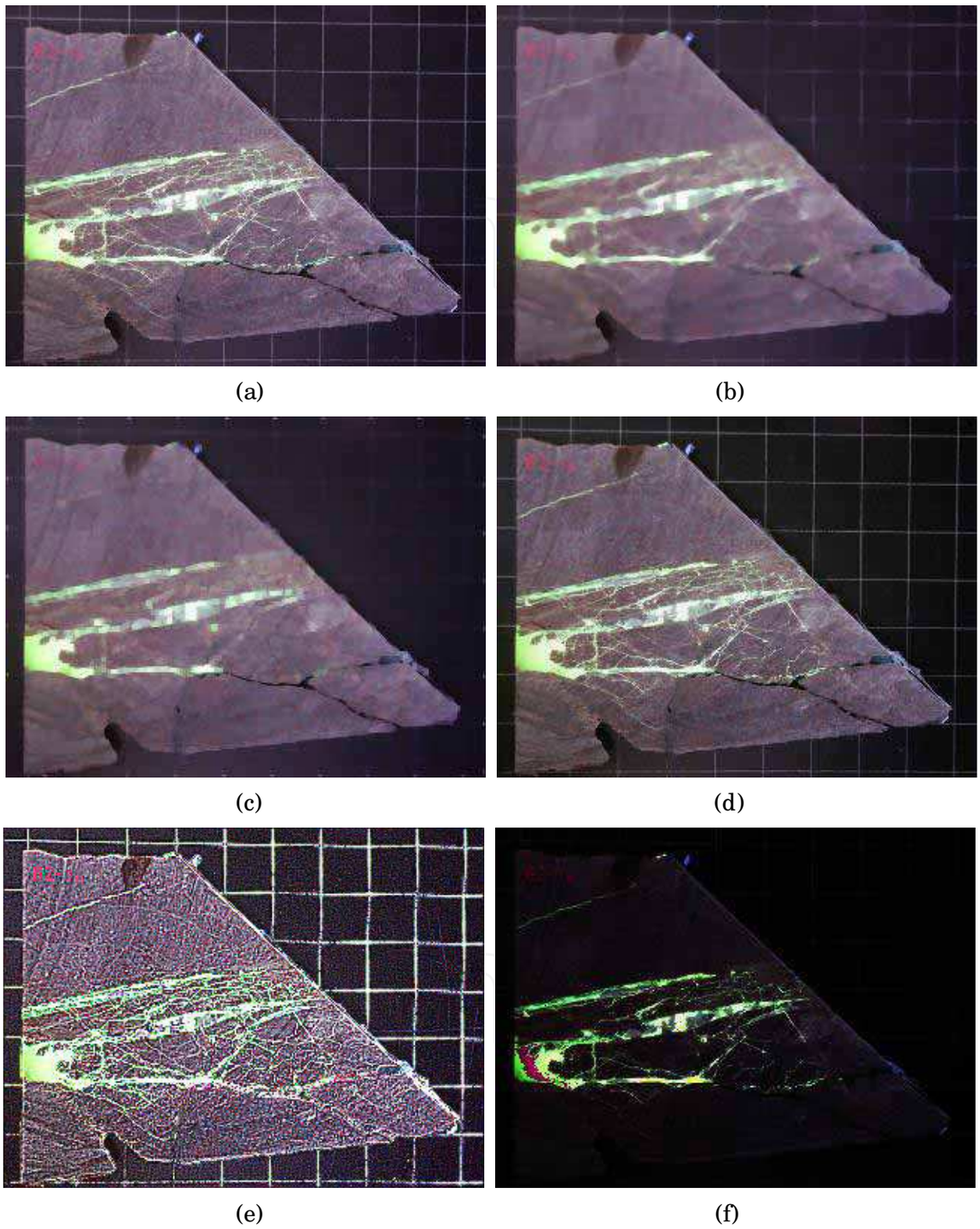

(a) (b)

(c) (d)

(e) (f)

Fig. 6. Comparison of image preprocessing operators: (a) Original image; (b) Median filter; (c) Morphological operation; (d) Linear stretch; (e) Sharpening; and (f) Exponent transformation.

The content of this part is (1) to compare the selected four of widely used global thresholding algorithms for four typical fracture images; (2) based on the comparison, to see how they work for rock fracture images, and (3) how to choose a global thresholding algorithm to segment the rock fracture images with a small variable background (the background is not completely uniform).

3.1.1 Thresholding algorithms selection and implementation

Thresholding is one of the old, simple, popular and most important approaches to image segmentation. From literature review, the thresholding algorithms can be classified thresholding algorithms into two groups / 26-33/ . One is based on the characteristic feature (e.g. gray level) histogram. Another is based on gradient (or Laplacian) of an image. The main global thresholding algorithms they summarized include: Optimal thresholding (OPT), Between class variance (BCV), Entropy, Moment preserving, Bi-modes (the threshold is a valley point between main two peaks) - we called it as BIM, Edge based thresholding (DIFF), dynamic edge based thresholding (DYN. Lee and Chung 1989 / 28/ , evaluated five of the global thresholding algorithms, the five algorithms are OPT, BCV, Entropy, Moment preserving and Quadtree. They gave a conclusion that Entropy and Quadtree are sensitive to image characteristics such as contrast and histogram distribution.

In order to evaluate these global algorithms (abbreviated OPT, BCV, BIM, DYN, and DIFF), how available they are for rock fracture images, the algorithms have been implemented into a PC computer. As a sever to readers comprehensively understanding the comparison between the algorithms, a brief description of these algorithms are listed as the follows.

Notation: an image $f(x,y)$ has gradient magnitude image $g(x,y)=\left|\nabla^2 f(x,y)\right|$, and the histograms $hisf(i)$ and $hisg(i)$ are corresponding to $f(x,y)$ and $g(x,y)$ respectively.

(1) OPT [30]: Suppose that an image contains two values combined with additive Gaussian noise. In addition of knowing the area percentage of objects, the mean values and their standard deviations are also known, the thresholding value can be obtained through an optimizing way. The implemented algorithm is iterative (optimal) threshold selection, which can be found in [30].

The details can be summarized as:

Pre-set a threshold T, separate an image into objects and background, then use Eq.(1) to obtain a threshold. Repeat the steps until $T^{t+1}=T^t$, T^t is the threshold.

$$u_B^t=\frac{\sum_{(i,j\in Backgound)} f(i,j)}{TNBP},\quad u_O^t=\frac{\sum_{(i,j\in Object)} f(i,j)}{TNOP}$$

where , TNBP is the total number of background pixels, and TNOP is the total number of object pixels.

$$T^{t+1}=\frac{u_B^t+u_O^t}{2}$$

In our case: $T^{t+1}=0.4u_B^t+0.6u_O^t$.

(2) BCV[31]: The method supposes that the probability for each gray-level is p_i, mean value $\mu=\sum_{i=1}^{m} ip_i$. The image is divided into two parts (i.e. background and objects foreground),

one has gray-levels from 1 to k, probability $\omega_0 = \sum_{i=1}^{k} p_i = \omega(k)$, mean gray value $\mu_0 = \sum_{i=1}^{k} ip_i = \mu(k)/\omega(k)$, the another from $k+1$ to m, probability $\omega_1 = \sum_{i=k+1}^{m} p_i = 1-\omega(k)$, mean gray value $\mu_1 = \sum_{i=k+1}^{m} ip_i = \left(\mu - \mu(k)\right)/\left(1-\omega(k)\right)$, and $\omega_0\mu_0 + \omega_1\mu_1 = \mu$. Try to find maximum variance which is a function of variable k:

$$\sigma^2(k) = \omega_0(\mu_0 - \mu)^2 + \omega_1(\mu_1 - \mu)^2 = \omega_0\omega_1(\mu_1 - \mu_0)^2 = \frac{\left[\mu\omega(k) - \mu(k)\right]^2}{\omega(k)\left[1-\omega(k)\right]} \tag{1}$$

obtain corresponding k as thresholding value.

(3) DIFF[33]: Define that S is the set of pixels having gray level i, find maximum value

$$d = \sum_{(x,y)\in S} g(x,y) \tag{2}$$

and obtain the corresponding i is the threshold.

(4) DYN: It is the similar to the above algorithm, the difference is that the threshold value is not constant on the whole image; it varies from place to place. In this algorithm implementation, we used Canny edge detector first, then, divide the image into a number windows, the thresholds are obtained on the information of windows.

(5) BIM [26-27, 30]: After calculating the histogram of gray-level image, the lowest valley point between two major peaks is found as the thresholding value. The program implemented is: firstly smooth the histogram by using Guassian smoothing function (1,2,3,2,1), then detect the two main peaks by using gradient at each point of gray level histogram, finally search the valley point between two main peaks. The valley point can be detected as

$$G_l^k = hisf(k) - hisf(k-m),\ G_r^k = hisf(k) - hisf(k+m)$$

$$G^k = G_l^k + G_r^k \quad (G_l^k \rangle 0,\ \ G_r^k \rangle 0),\ T = MAX\left(G^k\right) \tag{3}$$

where, k=1,..., 256, threshold is corresponding to T. m is chosen by an operator, in the follows, we use m = 40.

3.1.2 Comparison between different global thresholding algorithms

In order to evaluate the performance of these five thresholding algorithms for rock fracture images, the test images were chosen based on (a) the images are the represents of fracture applications, and (2) fractures and background can be roughly distinguished by human vision (e.g. background is darker than fractures). Test images are of the size 320 by 240 uniformly quantified to 24 bits. Four typical images are shown in Fig. 7 and their histograms are shown in Fig.8 respectively. The image in Fig. 7a was taken from a slice, with two long fractures; its histogram is of a shape of a normal distribution. In Fig. 7b, the image is a microscope image with one fracture in details, and there are no two obvious peaks in the

histogram. In Fig. 7c, the image is a slice image, the background is rough; the many fractures form a network. The images in Fig. 7d is a round surface image, there is much noise on the image, and the fracture network is complicated. Figs. 8a-d show the histograms of the corresponding images in Figs. 7a-d. Most of the histograms seem to be ones of two modes, with two main peaks, but their shapes are very different.

One of the most difficult problems in comparing and evaluating the performance of thresholding algorithm is choosing a meaningful object performance criterion. The problem is that a criterion suitable for one application may not be suitable for a different application of thresholding techniques. However, the most important concern is the accuracy in segmentation of fracture images. In evaluation of the performance, the probability of error (or maximum shape) and uniformity, which are often observed by human vision, could be set as criteria.

In this study, it is not supposed to threshold each of the test images perfectly, the evaluation is based on comparing to human vision. The test results could be used for the fracture analysis in this work stage.

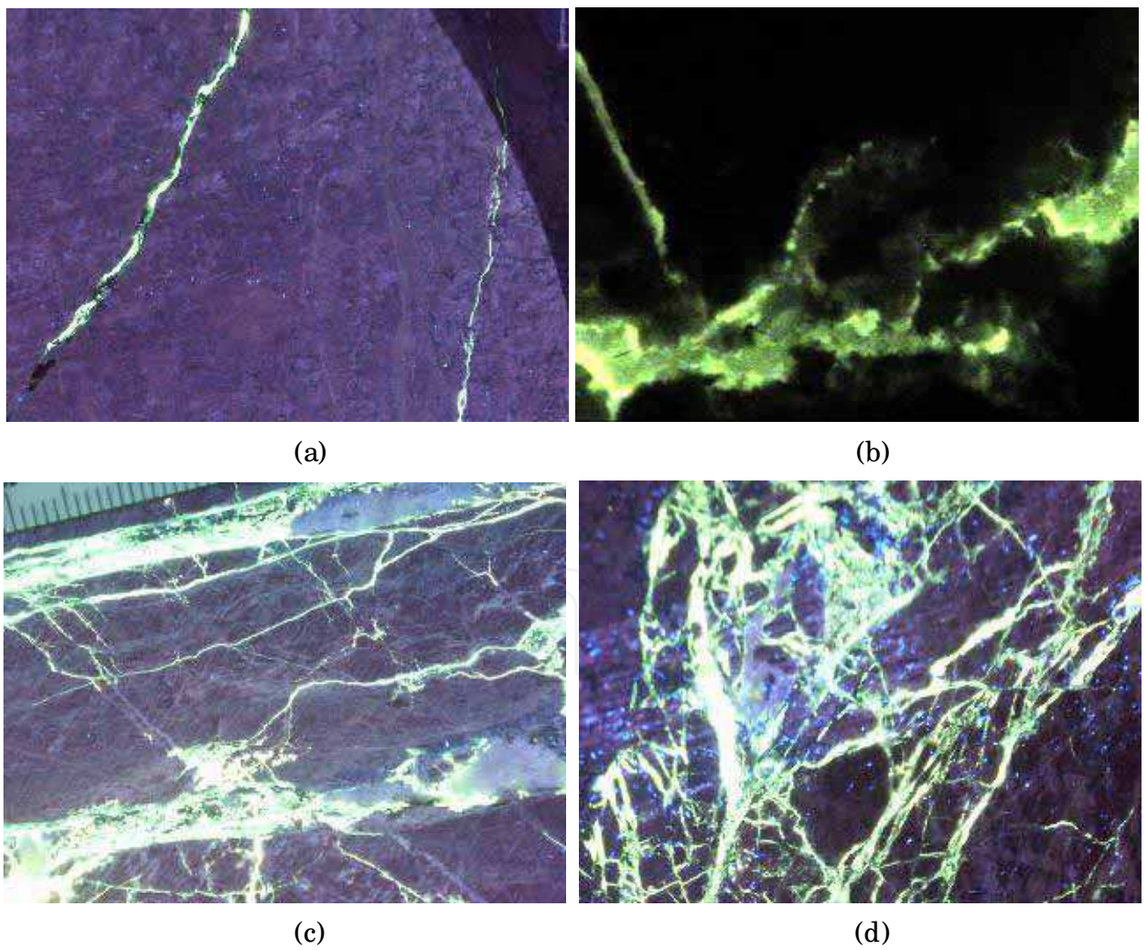

Fig. 7. Four typical rock fracture images.

As tested many times, OPT and BVC operations will give a similar result on any of our rock fracture images, therefore, in the figures 9-12, we just give OPT, BIM, DIFF and DYN operation results on each image in Fig. 7 for comparison. The testing results show (Fig. 9-Fig. 12) that OPT works on all the four images, BIM works on the image of a two modes (peaks) histogram, DYN may work for the images with complicated fracture network, and DIFF is sensitive to the information variation of rock fracture images.
Based on this testing result, we used OPT or BVC for all the rock fractures. The figure 13 demonstrates other four typical image thresholding results by using BVC thresholding algorithm. It is satisfied for our rock fracture images binarization, by using BVC or OPT.

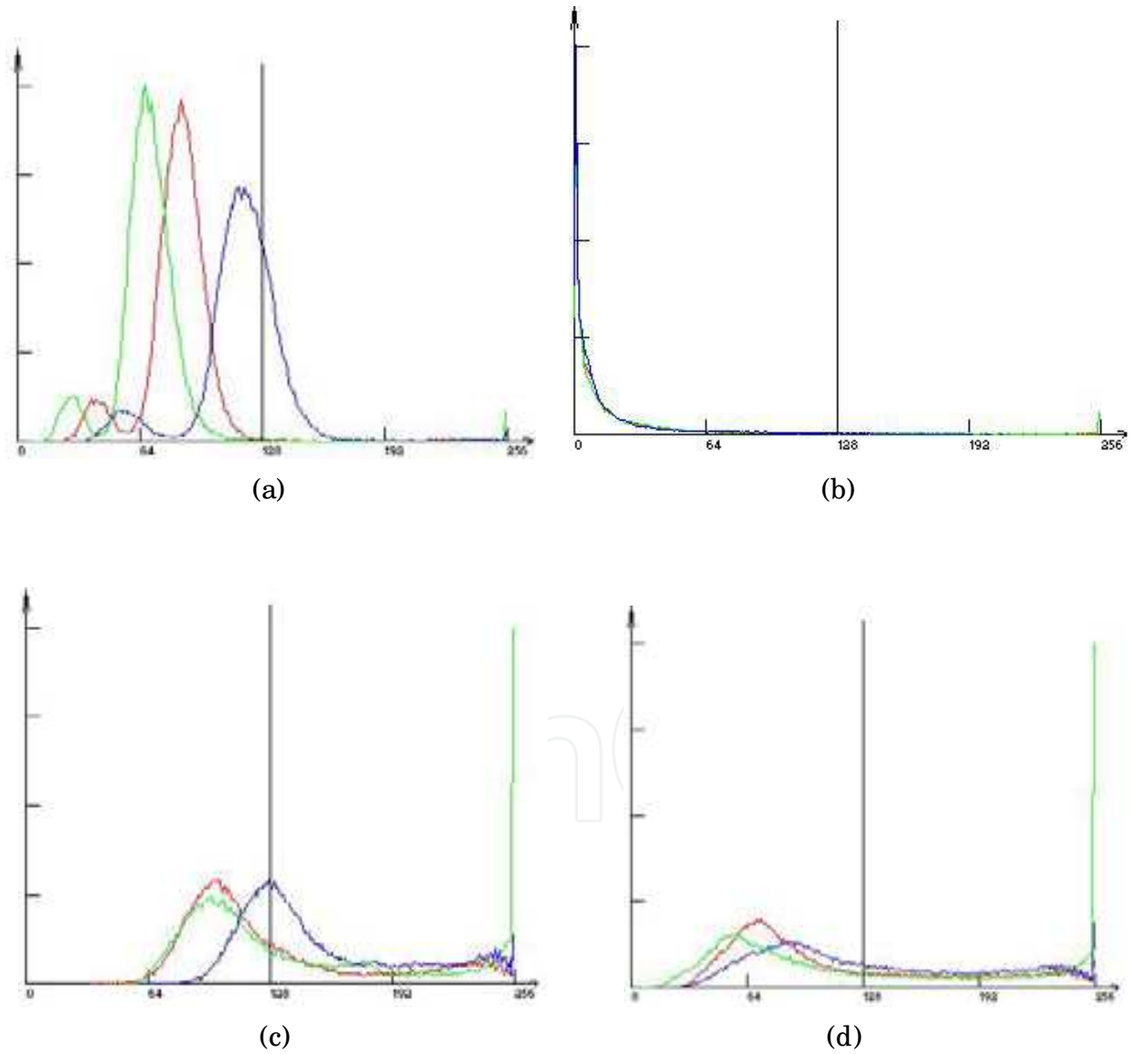

Fig. 8. Histograms for the images in Fig. 7 respectively.

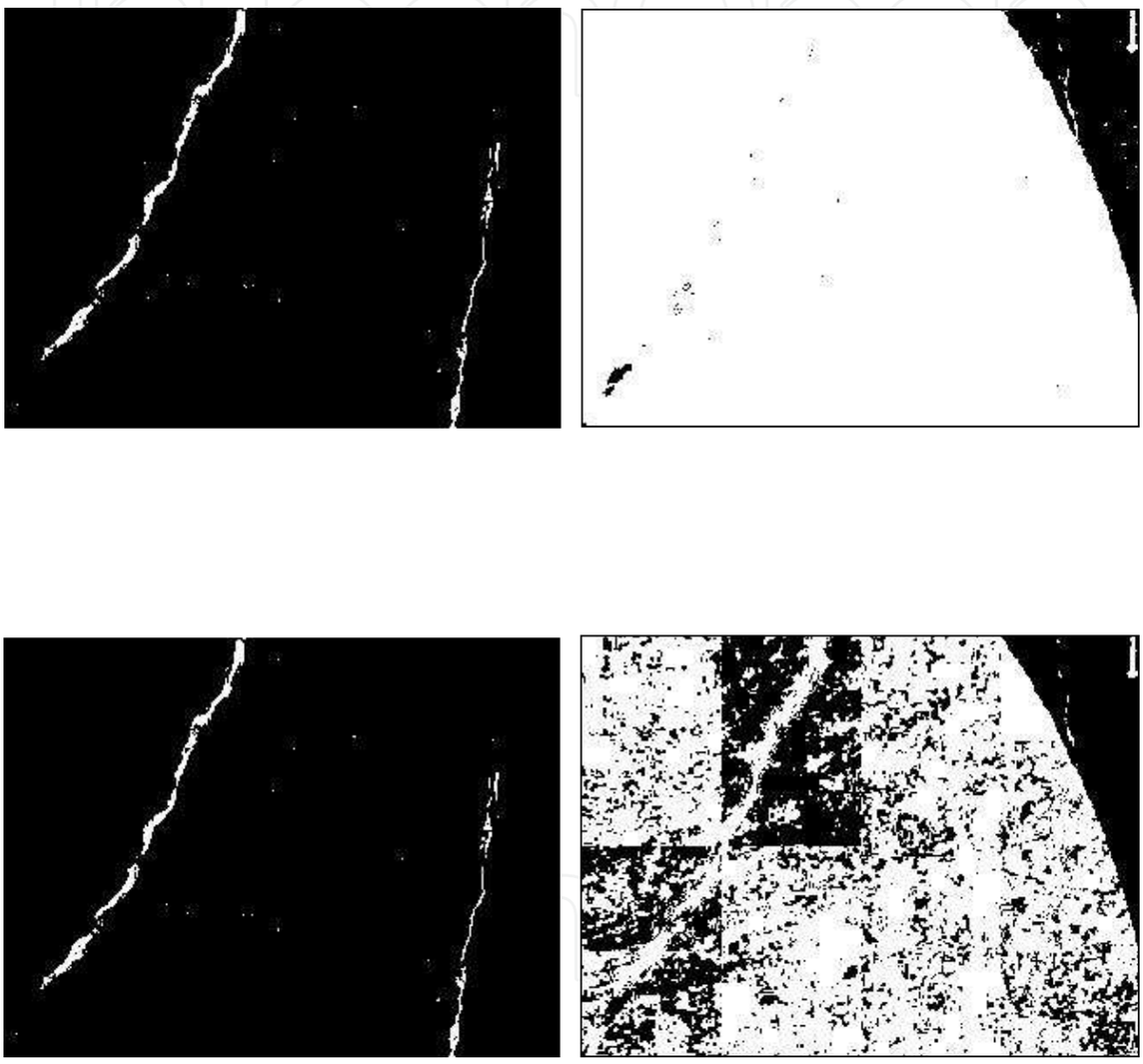

Fig. 9. Four threholding algorithms on the image in Fig. 7a: BIM and DYN are failed.

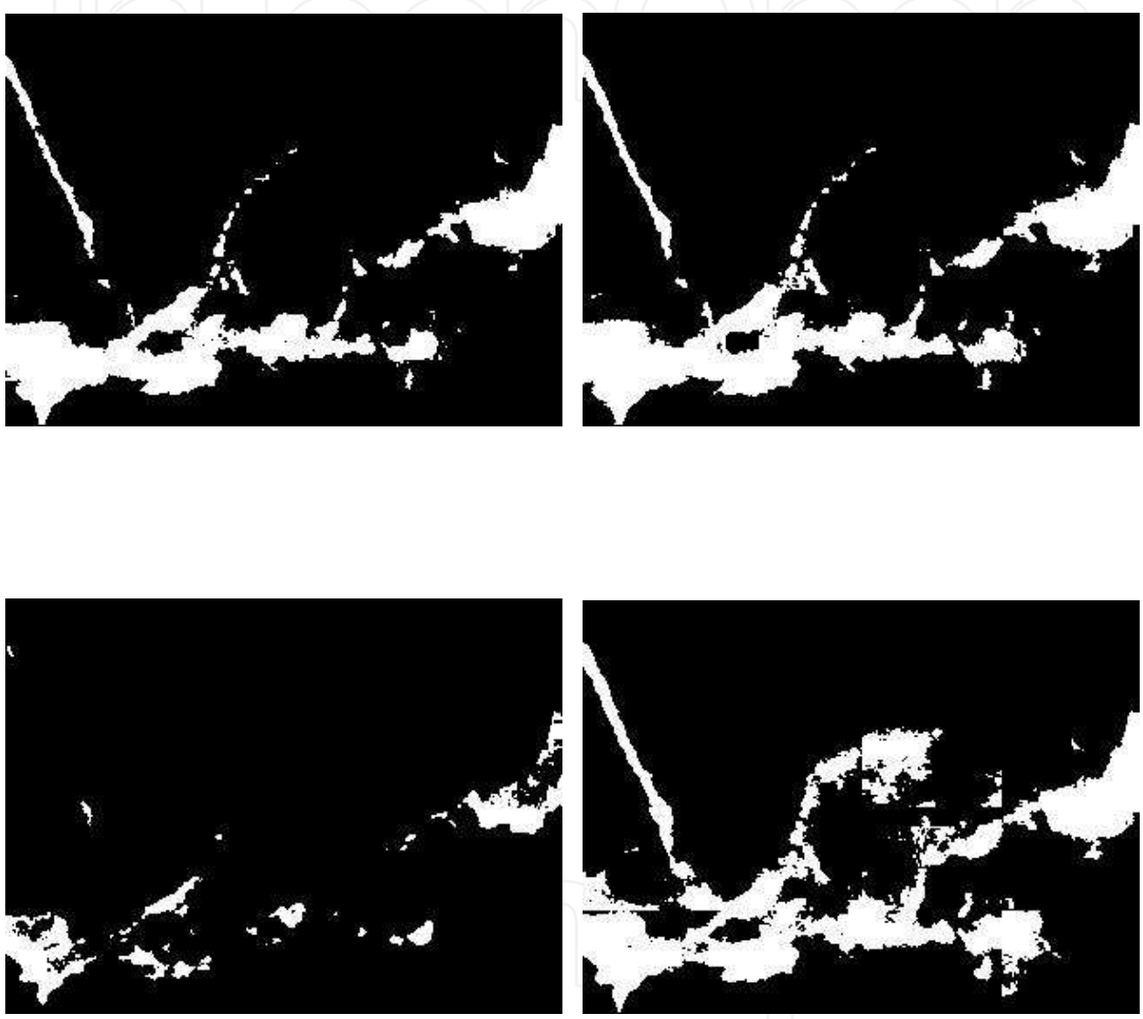

Fig. 10. Four threholding algorithms on the image in Fig. 7b: DIFF is failed, and DYN gives a larger fracture area than human vision detection.

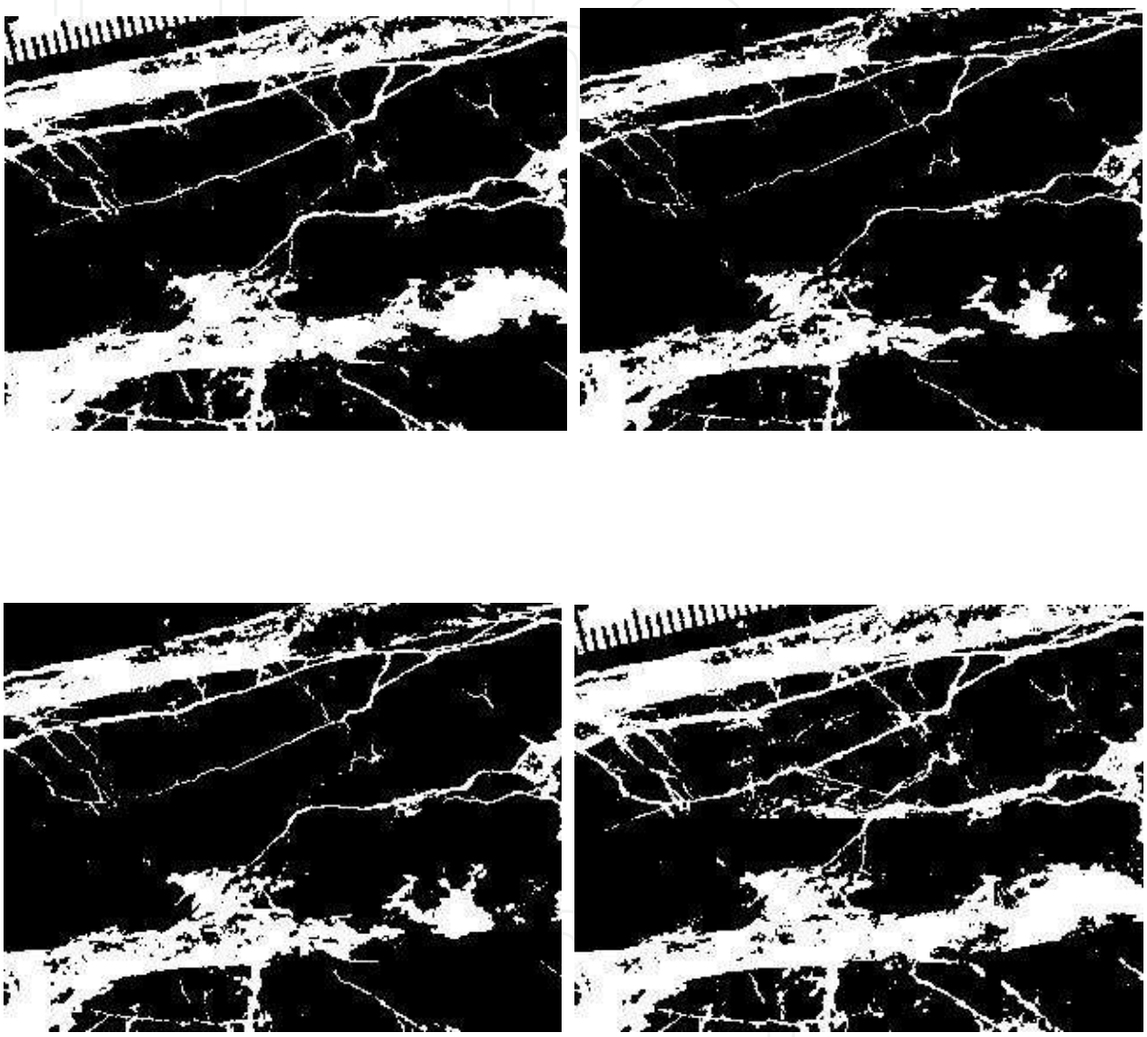

Fig. 11. Four threholding algorithms on the image in Fig. 7c: All the operations are seemed to be fair except for the scale ruler affection.

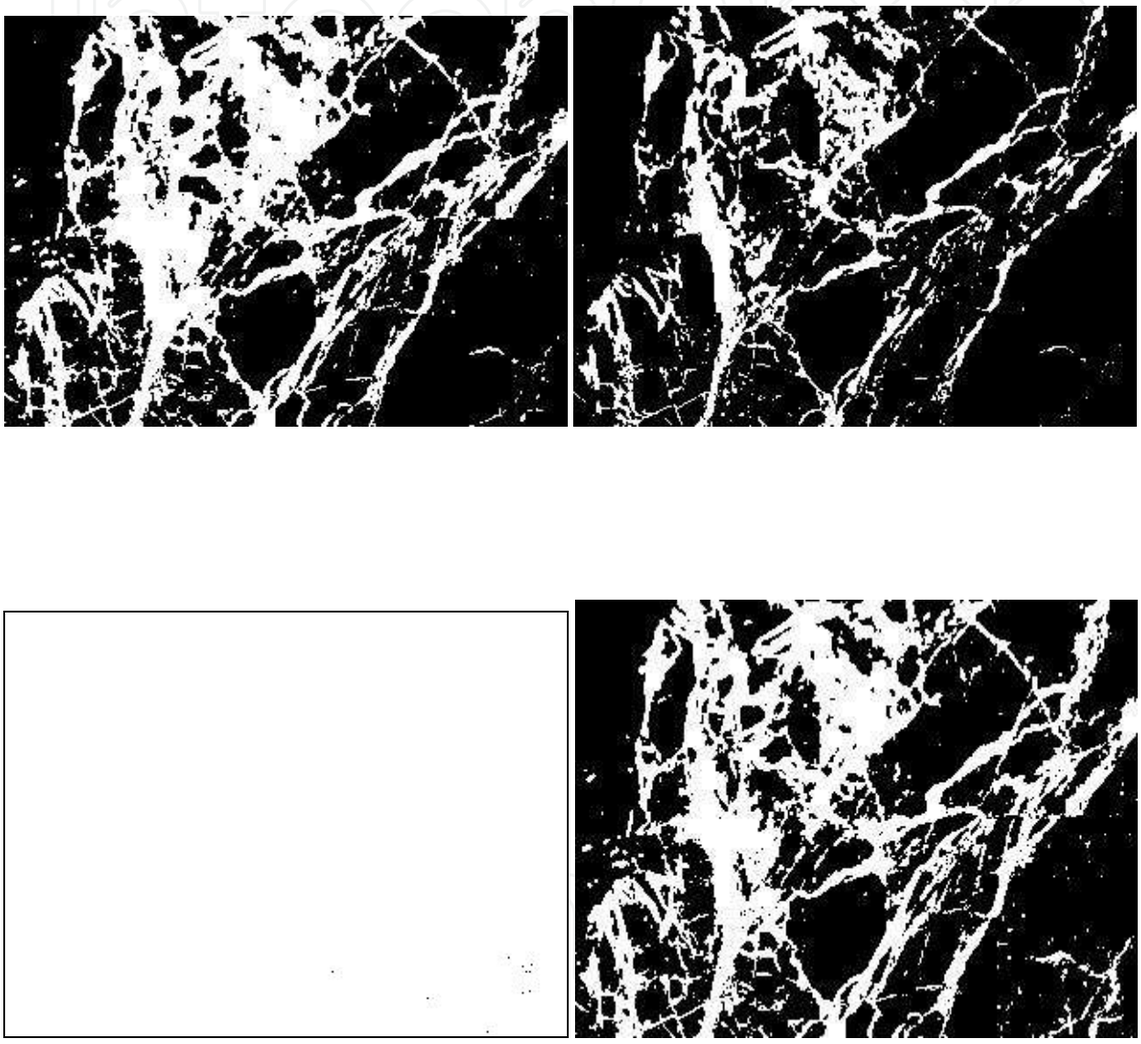

Fig. 12. Four threholding algorithms on the image in Fig. 7d: DIFF fails completely.

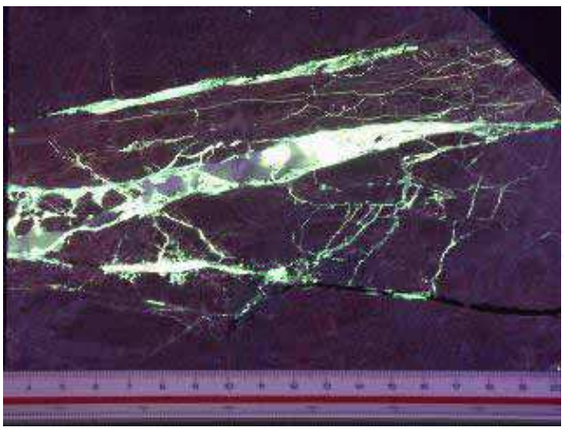

(a)

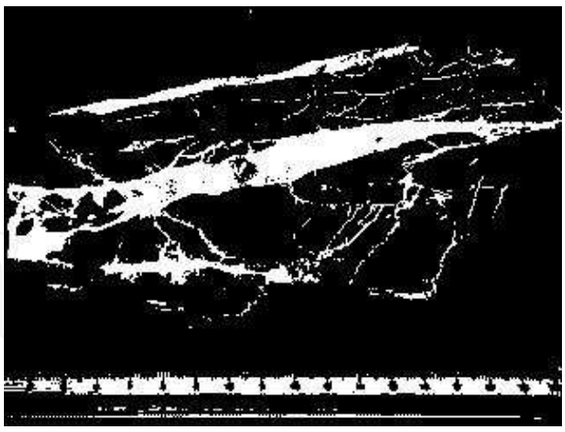

(b)

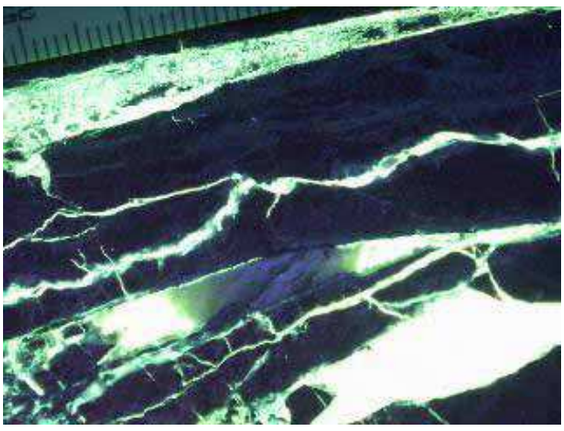

(c)

(d)

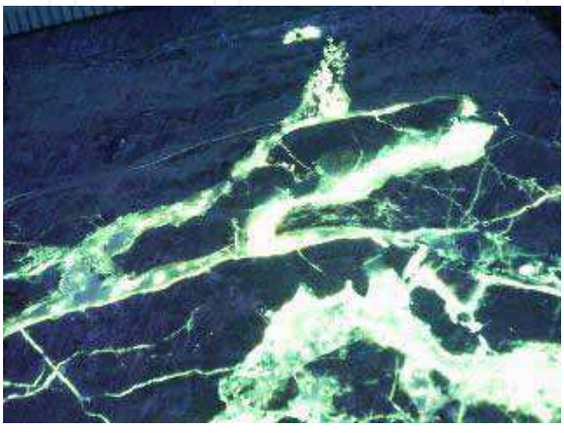

(e)

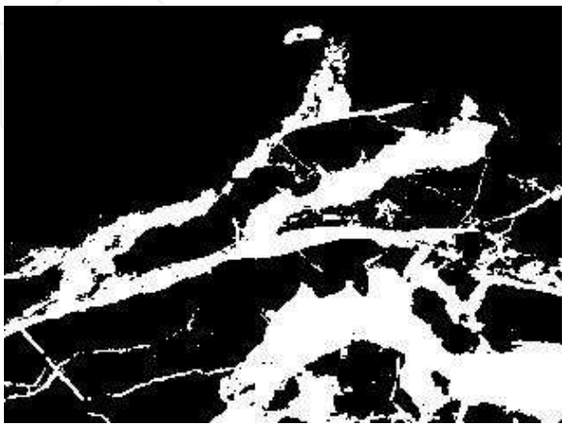

(f)

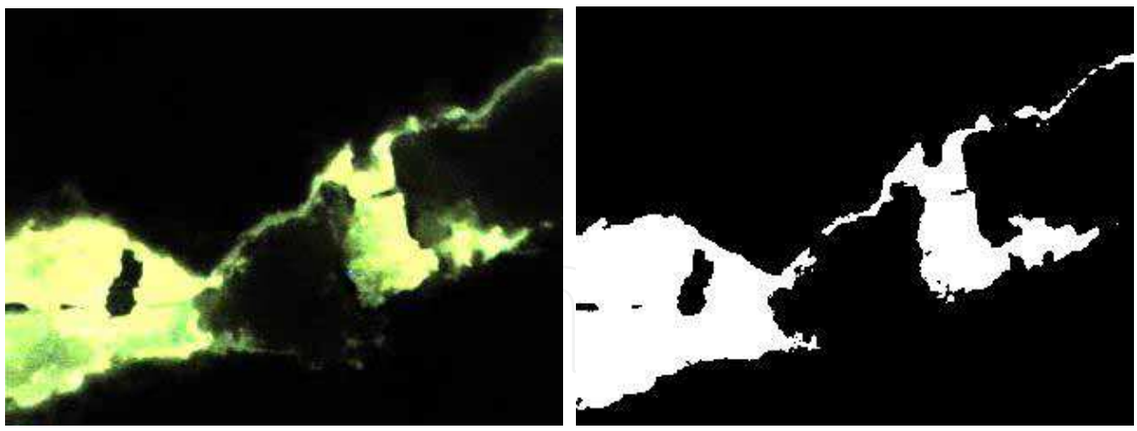

(a) (b)

Fig. 13. BVC algorithm on the four typical rock fracture images.

3.1.3 In conclusion

For a rock fracture image with a rather uniform background, and the range of the grey levels of fractures being not too large, the algorithms OPT and BCV are good choices for performing global thresholding.

In this study, a simple BIM algorithm is given, the test results show that it works for some kinds of images (the histogram consists of two main peaks); the algorithm design depends strongly on the types of histograms of fracture images.

For the fracture images, it is not suggested to use the thresholding algorithms based on gradient magnitude. The textured surfaces of the fractures will strongly affect the thresholding results although the background of images is rather uniform.

In general speaking, thresholding algorithms can be classified into manual, semi-automatic and automatic thresholdings. The automatic thresholding algorithms can be sub-classified into (1) the grey level histogram based and (2) based on the histogram of gradient magnitude. In the application of fracture recognition, if the images can be binarized satisfactorily by human vision, OPT and BCV are suggested to use for automatically thresholding. For the complex fracture images, adaptive thresholding algorithms maybe applied, in which, OPT and BCV are also suggested to use as a basis if needed.

To more accurately binarize the rock fracture images, adaptive thresholding, edge based or region based algorithms maybe needed to study. As a literature review, in recent years, many researchers recognized that it is difficult to use a single image segmentation algorithm to segment images in most of applications; the new focus topic is the fusion of different image segmentation techniques or algorithms. To do this kind of tests, we have developed some algorithms based on edge detection and region based (Fig. 14), the developed algorithms are useful for fracture tracing in some cases, the fusion procedure maybe next step development. In the next section, we will introduce our edge based segmentation idea.

3.2 Edge based segmentation algorithm

We here use gray-scale information (a color band) to trace the fracture curves. To develop the algorithm, several aspects must, generally speaking, be considered: (a) gray flatness or smoothness; (b) curvature variation; (c) magnitude strength; (d) computational searching costs; and (e) distance linking etc.

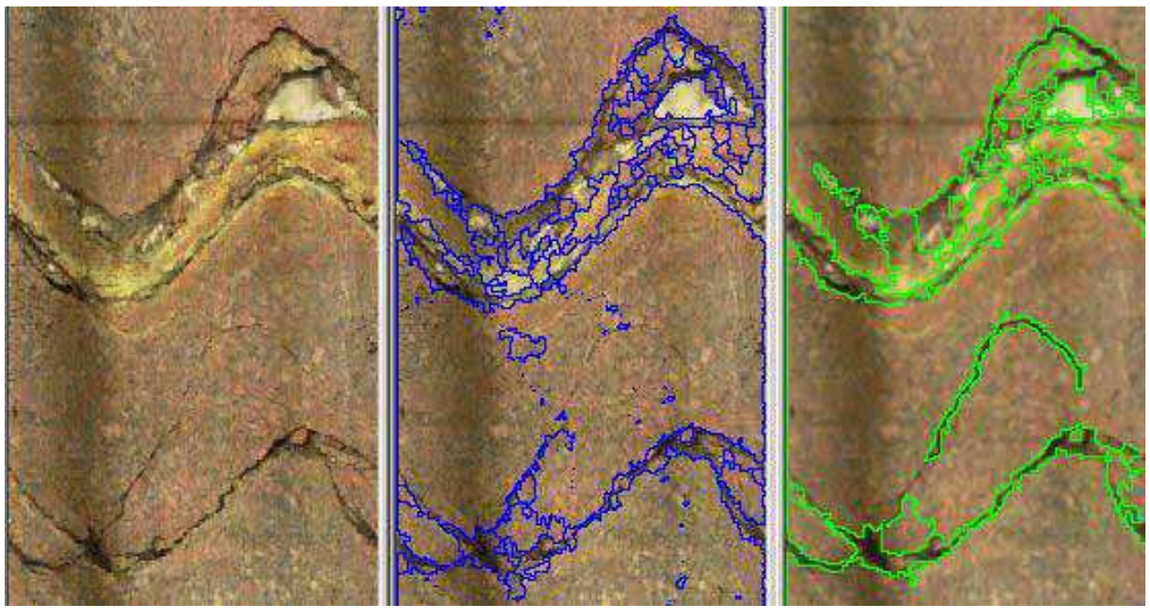

Fig. 14. Example of region based algorithm. Fracture tracing possibility for BIP images: Blue One is segmented based on image shrink, similarity (12, 80), and green one is segmented based on smoothing and similarity (7, 80). These are examples, for real segmentation, it need to modify the segmented fracture curves, e.g. to use triangle signal information, curve smoothing, small region merge and gap links. All these are post-processing, if the primary segmentation results can be like in the images, remaining tasks will be fixed anyway.

On the surface of rock mass, the objects of fracture often appear as step edges or ridge edges. The aim of image processing and image segmentation is to auto-tracing rock fractures, which is one of the most difficult tasks in image processing and image segmentation, due to the complicated properties on the rock surface.

Segmentation algorithms for monochrome images are generally based on one of two basic properties of gray-level values: discontinuity and similarity. In the first category, the approach is to partition an image based on abrupt changes in gray level.

An edge, in the image analysis literature, is a jump in intensity. The cross section of a so-called ideal edge has the shape of a ramp: infinite slope and flat portions on either side of the discontinuity. In smoother versions of the ideal edges, the first derivative (in appropriate direction) assumes a local maximum at a so-called edge point or edge pixel. A well-known edge detector of this type is the Canny edge detector, locating local maxima in gradient magnitude (=steepest slope). However, in our case we are more interested in another class of detectors, for example, those known as *ridge detectors* in the image analysis literature. A ridge can be simply thought of as a double edge (a bar edge). Between the step parts there is a narrow plateau or peak.

Sometimes, ridge detectors are expressed as follows: a bright (dark) ridge point is defined a point for which the intensity assumes a local maximum in the main principal curvature direction.

3.2.1 Ridge detection

The reported valley-edge detection algorithm in Wang and Bergholm (2003)/ 34/ , may be used as a ridge detector. A valley-edge detector tries to detect the lowest valley point in a

certain direction. If it is, the pixel is used as the valley-edge candidate, and its direction and location are marked, for further processing to form a valley-edge, by thinning and tracing procedures.

In Fig. 15a-b, when examining a pixel *p*, check the four different directions shown in the figure, to determine whether *p* is the valley-edge point or not. As an example, a small kernel valley-edge detection function runs as follows:

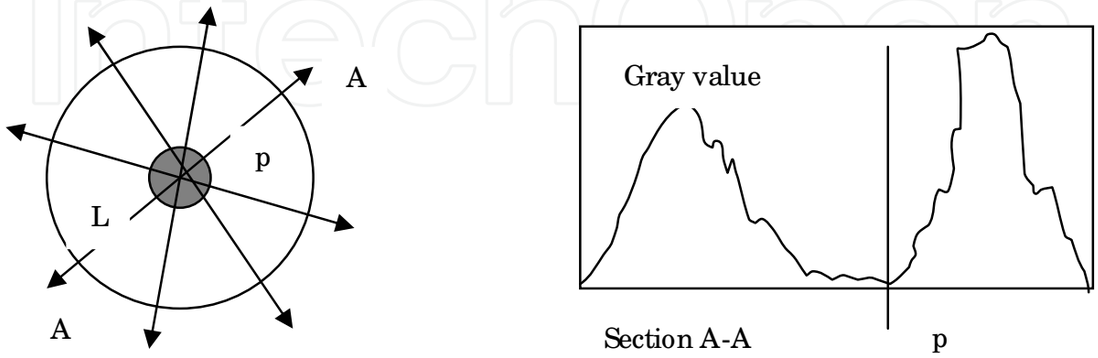

Fig. 15. The diagram for valley-edge detection algorithm, Wang and Bergholm (2003).

In the 0^o direction:

If $f(x,y) < f(x-1,y)$, then $F_1^0 = f(x-1,y) - f(x,y)$,

If $f(x,y) < f(x+1,y)$, then $F_2^0 = f(x+1,y) - f(x,y)$,

If $f(x-1,y) < \alpha f(x-2,y-1) + \beta f(x-2,y) + \gamma f(x-2,y+1)$, then

$F_3^0 = \alpha f(x-2,y-1) + \beta f(x-2,y) + \gamma f(x-2,y+1) - f(x-1,y)$,

If $f(x+1,y) < \alpha f(x+2,y-1) + \beta f(x+2,y) + \gamma f(x+2,y+1)$, then

$F_4^0 = \alpha f(x+2,y-1) + \beta f(x+2,y) + \gamma f(x+2,y+1) - f(x+1,y)$;

And similar expressions in the 45^0, 90^0 and 135^0 directions.

In the directionθ, calculate the following sum:

$$T_\vartheta = w_1 F_1^\vartheta + w_2 F_2^\vartheta + w_3 F_3^\vartheta + w_4 F_4^\vartheta$$

$\theta = 0^0$, 45^0, 90^0 and 135^0 ; w_i(i=1,2,3,4) are weights, e.g. $w_1 = w_2 = 1.2$, $w_3 = w_4 = 0.8$.

$T_{max} = \max(T_O, T_{45}, T_{90}, T_{135})$. If T_{max} is greater than a threshold T, the detected point will be marked as a valley-edge candidate.

The distance *L* (in the above formula, *L* = (i+1)-i = (j+1)-j=1)) is pre-determined based on image resolution and quality, and smoothing is done prior to valley-edge detection.

The details of the algorithm can be found in Wang et al. (2003)/ 34/ , here we merely stress that for each direction two values are calculated, and two values are obtained, f1 and f2 (=two 2nd differences at two scales). A weighted sum of these (in e.g. the 135 degree direction) is:

After valley-edge detection, a post-processing subroutine must be added. In the post-processing subroutine, several functions are used, such as thinning, bridging of small gaps, and removal of short curves or lines (refer to Figs. 16-17).

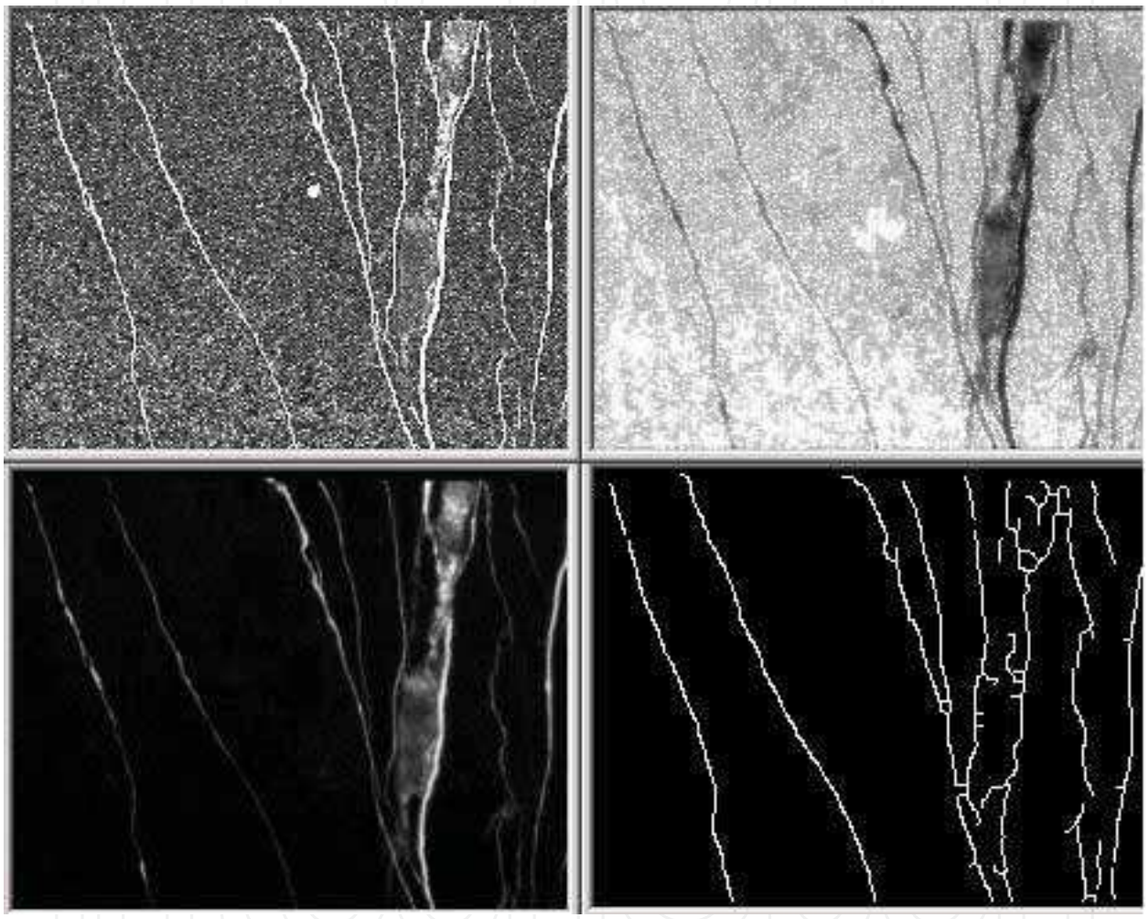

Fig. 16. Example 1 of fracture tracing by the new algorithm. The top-left image is original image, the top-right image is inverted and enhanced image, the bottom-left image is a magnitude image by Robert edge detector, and the bottom-right image is the result image.

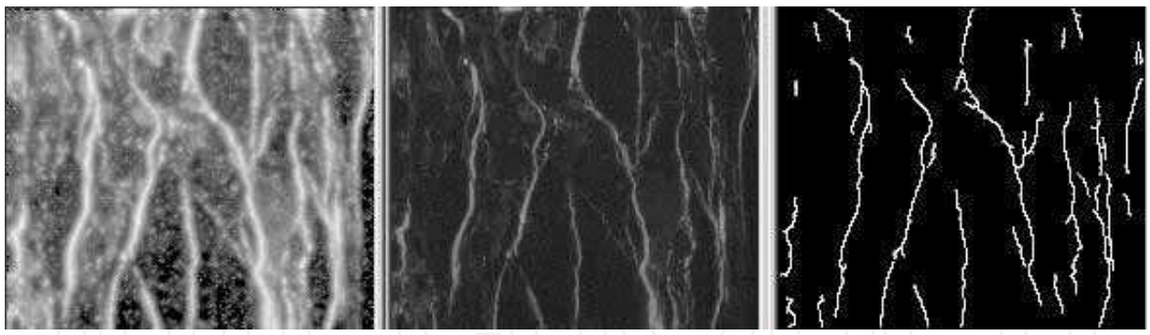

Fig. 17. Example 2 of fracture tracing by the new algorithm. The left image is original image, the middle image is a magnitude image, and the right image is the result image.

3.2.2 Multiple scales

Multi-scale representations are more or less related to scale-space theory, notably the theories of *pyramids*, *wavelets* and *multi-grid methods*. We will not describe and discuss the theory, the detailed information can be found in / 35-37/ . For the complicated rock fracture images, the methodology is very useful as we tested.

If most fractures in an image are very thin, the fine-detail information in the image is very important for fracture tracing, and the algorithm must avoid destroying the information. On the contrary, if fractures are thick, it is necessary to remove the detailed information on the rock surface, because it may produce a lot of fault fractures. In general, it is an image processing tool that the multiple scale technique makes image structures at coarse scales corresponding to simplifications of corresponding structures at fine scales.

By using the knowledge of multiple scales, we combine the valley edge detection results of different scale images, and have a promising fracture tracing result which is difficult to be obtained by using other methods. A gray scale fracture image of 734x596 pixels is presented in Fig. 18(a); its fracture tracing result is in Fig. 18(b). In Fig. 18(a), the noise edges randomly distributed on the whole image surface, and thick fracture cannot be detected properly by

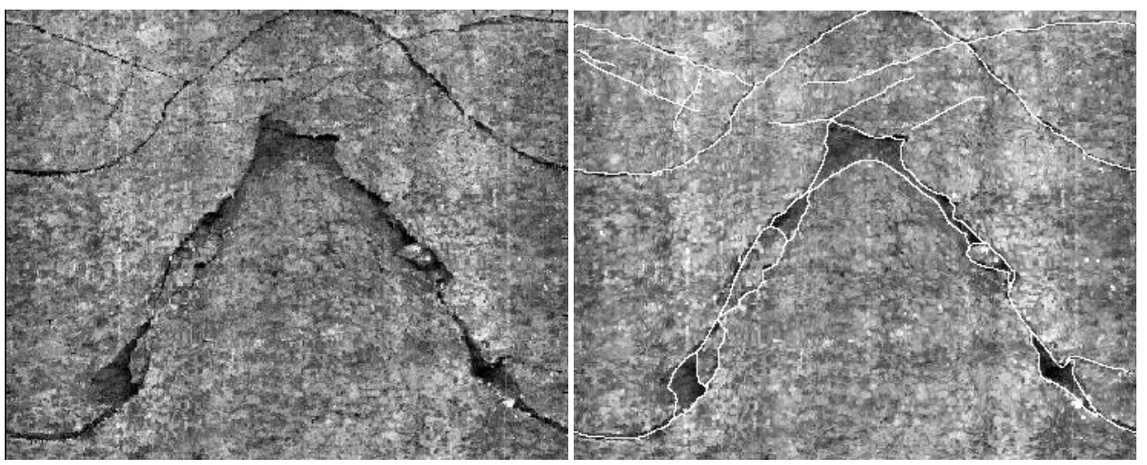

(a) (b)

Fig. 18. One example of rock fracture images: (a) Original image of resolution 734x596; and (b) Fracture tracing result.

using just valley edge detection. The fracture mapping result is processed based on the combination of multiple scales and our valley edge detection methods. The question is how to scale the image into different scale levels here, in the following; we will give a brief description of the question.

The image scale is reduced. Let $x = 1,...,n$, $y = 1,...,m$, and $f(x,y)$ is the original image. Then

$f(x_k,y_k)$, $x_k = 1,...,n/\ 2^k$, $y_k = 1,...,m/\ 2^k$, k = 1, 2, 3, 4,…

where, $k \le K$, $m \ge 2^K$, $n \ge 2^K$

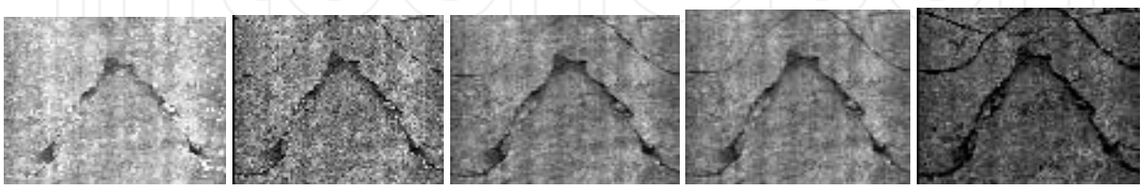

(a) (b) (c) (d) (e)

Fig. 19. Shrink image three times on the image in Fig. 18(a): (a) Maximum filter; (b) Odd lines; (c) Average filter; (d) Middle filter; and (e) Minimum filter.

To obtain valuable scaled $f(x_k,y_k)$, we tried several image shrink methods (e.g. used Gaussian, average, medium, adaptive, maximum and minimum etc. filters). The figure 6 is one of the examples to show the differences among the rock fracture image shrink methods. In figure 19, since fractures in Fig. 18(a) have low gray values, Maximum filter (in original image, choose maximum gray value pixel, of four neighboring pixels, as a new pixel in the shrink image) eras thin fractures, on the contrast, Minimum filter make fractures sharpen, but the noise are sharp too. In our case, we use Minimum filter to shrink image for three times, then smooth the scaled image by a Gaussian filter.

One of typical examples is shown in Fig. 20. The original image has a rough surface with thick fractures, if the developed ridge detection and fracture tracing algorithms are directly used without image scale operations, the detection result will include a lot of fault fractures. When we shrink the original image one time, the detection result will be better. The best detection result is in Fig. 20(d), where, we shrink the image for three times before ridge detection and fracture tracing.

3.2.3 In conclusion

For this study, we have developed a number of algorithms for image processing and segmentation, especially for rock fracture images. The presented fracture detection algorithm is the robust for ridge edge detection and fracture tracing, but for the rough surface with thick cracks or fractures, using multi-scale technology can allevate producing noise fractures. The next step of work is to use nural network and statistics / 38-41/ to calssify images into different classes, then use pyramid methods to divide original image into several scale levels, to use the detection algorithm with different parameters to detect fractures.

3.3 Fractional differential algorithms

It is a new research topic that fractional differential theory is used into image processing. We a new type of algdeveloped new algorithms to improve the fractional differential Tiansi

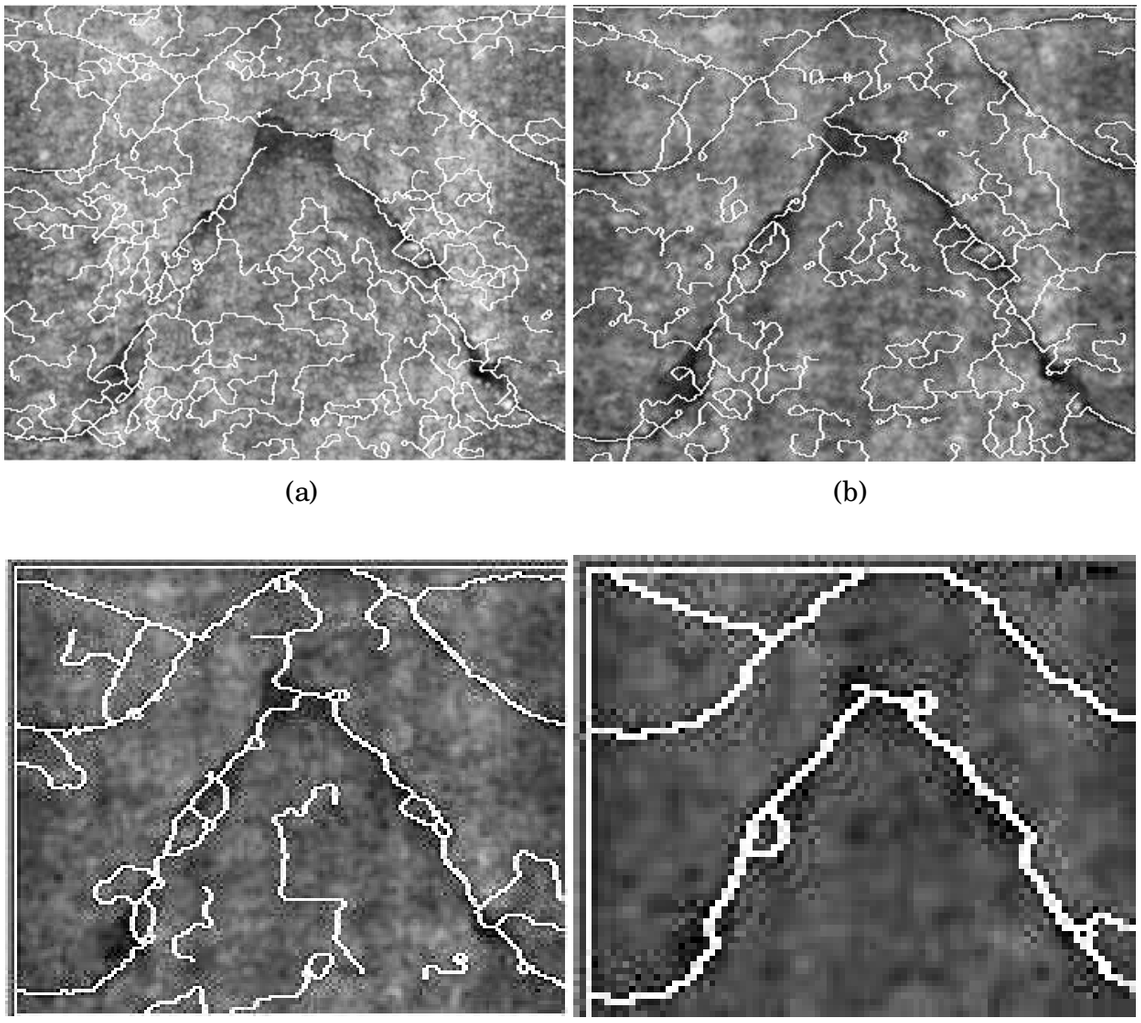

Fig. 20. Valley edge detection result: (a) Image of resolution 734x596; (b) Image of resolution 367x298; (c) Image of resolution 183x149; and (d) Image of resolution 91x74.

operator, which can significantly enhance the edge information. The studied algorithms are based on the enhancement ability of fractional differential to rock fracture image details, and they can be used to analyze the mechanism of fractional differential. The general procedure of the algorithms is as follows: Firstly, Tiansi template is divided into eight sub-templates with different directions around the detecting pixel, and then eight weight sum values for the eight sub-templates are obtained. Furthermore, those eight weights are classified into different groups. In this way, the three improved algorithms with different enhancing ranges are obtained. Finally, the experiments of edge enhancement show that the improve algorithms can enhance edge information more effectively and can show much more detailed information

than traditional edge detection operators especially for the image segmentation of complicated rock fracture images. The detailed information can be found in reference [42].

3.4 Rock fracture detection based on quaternion convolution by scale multiplication

In order to suppress the noise, the dot product is computed at adjacent scales. At the same time, we apply gray-level difference to obtain the monochromatic edges. To merge the merits of the quaternion convolution and the gray-level difference, the two results are used at the same time. Finally, the thinned edges can be obtained by using modulus maximum suppression. Experimental results show that the algorithm is efficient and robust for rock fracture edge detection.

In this study, we firstly presented the rock fracture image acquisition method. Since the width and color of the fracture vary much, it is usual that there are many gaps on one crack or fracture. This study use quaternion convolution for rock fracture edge detection. When the pixels are chromatic, the quaternion convolution is more efficient than other methods. At the same time, we use the gray-level image to obtain the monochromatic edge points. Then thinned edges can be obtained by using modulus maximum suppression. Experiment results show that the method is both efficient and robust. The detailed information is in reference [43].

3.5 Rock fracture edge detection based on Wavelet Analysis

Wavelet analysis is internationally recognized up to minute tool for analyzing time frequency. This study discusses the technique of image processing based on wavelet transform.

There are many methods to obtain the rock fracture images. The inner fractures image can be obtain using ultraviolet and the external fractures image can be obtain using visible light. The methods are efficient and low cost.

To detect the ultraviolet image fractures, we presented an algorithm based on multiscale wavelet transform. After obtain the gray scale images, the image can be split to three types of area: the black, the white and the transitional area. The edge detection can be enhanced and the noise can be reduced by scale multiplication. The method is useful not only for rock fractures detection but for other images edge detection.

The color images are acquired using visible light and the fractures are more complicated. This paper presents the fracture detection algorithm based on quaternion convolution. After the color image is convoluted using different scale quaternion operators, the dot product is applied. At last, the edge map is obtained using modulus maxima suppressed.

Because of the color image is noisy and the ultraviolet image is clear edge, the better idea is fuse the two types of images. After the color image is transformed to IHS color space, the edge information is fused in different areas. The fused image is more using for image processing. The interested readers can refer to [44].

3.6 Rock fracture tracing based on image processing and SVM

This study presented a new methodology for automated rock fracture trace detection, description and classification based on automated image processing techniques and support vector machine (SVM). The developed procedure uses a series of photographs of a rock face which were taken by sophisticated CCD cameras. All digital image are be processing by the

developed algorithm, and fracture traces extracted from the processed image are then identified and categorized by SVM. The proposed procedure has been tested by detecting fracture and classifying the fracture traces. Results show that the approach is useful and robust...

The aim of this study is to present a novel, automated and robust methods for rock fracture tracing. Image processing technology is used to get high quality of image segments for recognition. Support vector machine is introduced into the rock fracture classification for the first time in this field. Although the methods didn't achieve the expect performances, there are a lot of advantages compared with the current technology.

SVM is very promising to tackle complicated problems in rock fracture trace recognition and it could be enlarged to more complex structures in future research. As a reliable technique to identify fracture traces in practice, this method should be tested in more real measurement cases. And for further work, a SVM image segment and recognition system can be constructed. The detailed description for this study can be found in reference [45].

4. Conclusions and suggestions

1. For this study, we have developed and collected a number of algorithms for rock fracture image processing and segmentation.
2. A number image preprocessing algorithms have been discussed and compared.
3. Several auto-thresholding algorithms have been studied and compared, and the BCV or OPT algorithms are considered satisfactory for the rock fracture images in this testing stage roughly analysis of rock fracture network properties).
4. Except for the thresholding algorithms, a region based segmentation algorithm is also tested for BIPS images.
5. The developed edge detection algorithms are robust for ridge edge detection and fracture tracing. It has been tested for the images of single fracture and fracture network, it is promising, and it may need more tests further.
6. For difficult images (where cracks and fractures are difficult to distinguish due to either minerals or shadows etc.) and images with wide fracture apertures, using multi-scale technology can alleviate producing noise fractures.
7. The next step of work needs to create an auto preprocessing procedure to all the rock fracture images first, then, to modify the developed threhsolding, region based and edge based image segmentation algorithms, make them to fit for our rock fracture images respectively.
8. Finally to use neural network, fuzzy logic, wavelet/ 38-41/ and artificial intelligence technologies to classify images into different classes, then use pyramid methods to divide original image into several scale levels, to use the fusion of the different detection algorithms to setup a fracture image segmentation procedure, and to auto-detect rock fractures.

Anyhow, the different rock fracture images need different image segmentation algorithms. Since rock fracture images are so different that they cannot be segmented by only one image segmentation algorithm. In this chapter, eight different image segmentation algorithms are studied and developed for rock fracture images, one of the

algorithms is suitable for one or several types of rock fracture images, but not for all the types of images. In the future work, the algorithms will be further studied and tested, then, one image segmentation system will be constructed by several image segmentation algorithms that are selected based on a neural network system, for a processing image of rock fractures.

5. Acknowledgements

This research is supported by the Special Fund for Basic Scientific Research of Central Colleges, Chang'an University in China with number: CHD2010JC004.

6. References

[1] Liu H. et al., 2004, Characterization of rock heterogeneity and numerical verification, Engineering Geology, Volume 72, Issues 1-2 , March 2004, Pages 89-119.

[2] Laubach S. et al.,2004, Coevolution of crack-seal texture and fracture porosity in sedimentary rocks: cathodoluminescence observations of regional fractures, Journal of Structural Geology Volume 26, Issue 5 , May 2004, Pages 967-982.

[3] Chen S. et al., 2004, Digital image-based numerical modeling method for prediction of inhomogeneous rock failure Int. J. Rock Mech. & Min. Sci., 41, 939-957. Chen, S., et al. (2004).

[4] Zhou Y. et al., 2004, Segmentation of petrographic images by integrating edge detection and region growing, Computer & Geosciences 30 (2004) 817-831.

[5] Final report of the TRUE Block Scale project, 4. 2003 , Synthesis of flow, transport and retention in the block scale, March 2003, Swedish Nuclear Fuel and Waste Management Co. (SKB, Technical Report, TR-02-16).

[6] Lemy F., Hadjigeorgiou J., 2003, Discontinuity trace map construction using photographs of rock exposures, International Journal of Rock Mechanics and Mining Sciences, Volume 40, Issue 6 , September 2003, Pages 903-917.

[7] Lyman, G. J., 2003, Rock fracture mean trace length estimation and confidence interval calculation using maximum likelihood methods, International Journal of Rock Mechanics and Mining Sciences, Volume 40, Issue 6, September 2003, Pages 825-832.

[8] Kemeny, J., Randy Post, 2003. Estimating three-dimensional rock discontinuity orientation from digital images of fracture traces, Computer & Geosciences, v. 29 n. 1, p.65-77 February.

[9] Parviz S. et al., 2003 , Specimen preparation and image processing and analysis techniques for automated quantification of concrete microcracks and voids Cement and Concrete Research, Volume 33, Issue 12, December 2003, Pages 1949-1962.

[10] Jorge A., Lambros J., 2002, Investigation of crack growth in functionally graded materials using digital image correlation, Engineering Fracture Mechanics Volume 69, Issues 14-16 , September 2002, Pages 1695-1711.

[11] Reid T., Harrison J., 2000, A semi-automated methodology for discontinuity trace detection in digital images of rock mass exposures, International Journal of Rock Mechanics and Mining Sciences, Volume 37, Issue 7, October 2000, Pages 1073-1089.

[12] Johansson M., 1999, Digital image processing of borehole images for determination of rock fracture orientation and aperture, Licentiate thesis, at Division of Engineering Geology, Department of Civil and Environmental Engineering, KTH, 1999, TRITA-AMI LIC 2041.

[13] Trevor Raymond Reid, A methodology for the detection of discontinuity traces in digital images of rock mass exposures, Doctoral thesis, in the University of London (Imperial College of Science Technology & Medicine), 1998.

[14] Power W,. Durham W., 1997, Topography of Natural and Artificial Fractures in Granitic Rocks: Implications for Studies of Rock Friction and Fluid Migration, Int. J. Rock Mech. Min. Sci. Vol. 34, No. 6. pp.979-989, 1997.

[15] Feng Quanhong, Application of Image processing to borehole logging, master thesis, at Division of Engineering Geology, Department of Civil and Environmental Engineering, KTH, 1996.

[16] Hakami, E., 1995, Aperture Distribution of Rock Fractures, Doctoral thesis, at Division of Engineering Geology, Department of Civil and Environmental Engineering, KTH, 1995, TRITA-AMI PHD 1003.

[17] Masahiro Iwano, 1995, Hydromechanical Characteristics of a Single Rock Joint, Doctoral thesis, in Massachusetts Institute of Technology, 1995.

[18] Harrison JP, 1993. Improved analysis of rock mass geometry using mathematical and photogrammetric methods. Ph.D. thesis, Imperial College, London, UK.

[19] Hu J, Sakoda B, Pavlidis T., 1992. Interactive road finding for aerial images. IEEE Workshop on Applications of Computer Vision.

[20] Franklin, John A., Norberth H. Maerz and Caralyn P. Bennett, 1988. Rock mass characterization using photoanalysis, International Journal of Mining and Geological Engineering, pp. 97-112.

[21] Takahashi M. , Takemura T., 2004 , Microscopic visualization in rocks under confining pressure by means of micro focus X-ray CT, Proceedings of the ISRM International Symposium 3rd ARMS, Ohnishi & Aoki (eds) 2004 Millpress, Rotterdam, ISBN 90 5966 020 X, pp. 139-142.

[22] Sun, G. X., D. J. Reddish and B. N. Whittaker, 1992, Image analysis technique for rock fracture pattern studies around longwall excavations, Trans. Instr Min. Metall, Sect. A: Min. industry, v. 101, A127-204, London.

[23] Tanimoto C, Murai S, Kiyama Joshi AK. , 1989. Automatic detection of lineaments from Landsat data. Proceedings of the IGARSS'89, Vancouver, Canada.

[24] Zou Dingxiang, Weixing Wang and Ma Bailing, 1986. Computer simulation of spatial distribution of weakness planes and its influence on rock blasting, Proc. of the Int. Sym. on intense dynamic loading and its effects, in Beijing of China, pp. 1056-1062.

[25] Huang Kaiqi, Wu Zhenyang, Wang Qiao, Image enhancement based on the statistics of visual representation, Image and Vision Computing 23 (2005) 51-57.

[26] N. Otsu, A threshold selection method from gray-level histogram, *IEEE Trans. Systems Man Cybernet*, 1979, SMC-9, pp. 62-66.

[27] K.S. Fu and J.K. Mu, A survey on image segmentation, *Pattern recognition*, 1981, Vol. 13, pp. 3-16.

[28] N.R. Pal and S.K. Pal, A review of image segmentation techniques, *Pattern recognition*, 1993, Vol. 26, No. 9, pp. 1277-1294.

[29] K. Lee and S.Y. Chung, A comparative performance study of several global thresholding techniques for segmentation, *Computer Vision, Graphics, And Image Processing*, 1990, 2, pp. 171-190.

[30] A.M. Groenewald, E. Barnard and E.C. Botha, Related approaches to gradient-based thresholding, *Pattern recognition Letters*, 1993, Vo. l4, pp. 567-572.

[31] M. Sonka, V. Hlavac and R. Boyle, *Image processing, analysis and machine vision*, 1995, Champion & Hall, 2-6 , Boundary Row, London SEI 8HN, UK.

[32] W.H. Tsai, Moment-preserving thresholding: A new approach, *Computer Vision, graphics, And Image Processing*, 1985, 29, pp. 377-393.

[33] J.N. Kapur, P.K. Sahoo and A.K.C. Wong, A new method for grey-level picture thresholding using the entropy of the histogram, *Computer Vision, Graphics and Image processing*, 1985, 29, pp. 273-285.

[34] Wang, W.X. , Froth delineation based on image classification, International Journal of Mineral Engineering, Volume 16, Issue 11 , November 2003, Pages 1183-1192.

[35] Benoit Tremblais, Bertrand Augereau, 2004, A fast multi-scale edge detection algorithm, Pattern Regognition Letters 25 (2004) 603-618.

[36] Lindeberg, T., Detecting Salient Blob-Like Image Structures and Their Scales with a Scale-Space Primal Sketch: A Method for Focus-of-Attention, *International Journal of Computer Vision, 11(3), 283--318, 1993.*

[37] Sergios P., Stavros J., 2004, On the relation between discriminant analysis and mutual information for supervised linear feature extraction, Pattern Recognition 37(2004) 857-874.

[38] Manesh K. et al., 2004, Cosine-modulated wavelet based texture features for content-based image retrieval, Pattern Recognition Letters 25 (2004) 391-398.

[39] Munoz X. et al., 2003, Strategies for image segmentation combining region and boundary information, Pattern Recognition Letters 24(2003) 375-392.

[40] Egmont-Petersen M., de Ridder D., 2002, Image processing with networks- a review, Pattern Recognition 35(2002) 2279-2310.

[41] Anil K. et al., 2000, Statistical Patter Recognition: A Rview, IEEE Trans Pattern And Machine Intelligence, Vol. 22, No. 1, January, 2000, 4-37.

[42] Weixing Wang, Juan Wan and Yang Zhao, 2010, Rock Fracture Extracting on Fractional Differential, The 2nd International Workshop on Intelligent Systems and Applications (ISA 2010).

[43] Jiangyan Xu, Weixing Wang, Linning Ye, 2009, Rock fracture edge detection based on quaternion convolution by scale multiplication, Optical Engineering, 48(9), pp. 097001-(1-7) .

[44] Jiangyan Xu, Weixing Wang and Liwan Chen, 2007, An image fusion algorithm for rock fracture detection using wavelet transform, AOMATT 2007, Chengdu, August.

[45] Weixing Wang, Haijun. Liao and Ying Huang, 2007, Rock fracture tracing based on image processing and SVM, ICNC-FSKD 2007, Hainan, July 2007.

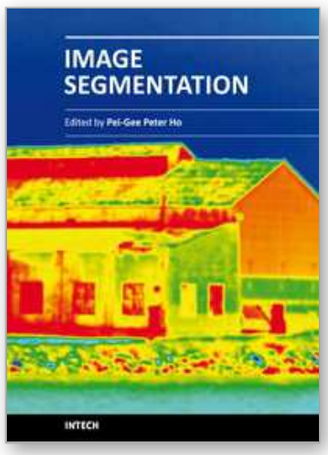

Image Segmentation
Edited by Dr. Pei-Gee Ho

ISBN 978-953-307-228-9
Hard cover, 538 pages
Publisher InTech
Published online 19, April, 2011
Published in print edition April, 2011

It was estimated that 80% of the information received by human is visual. Image processing is evolving fast and continually. During the past 10 years, there has been a significant research increase in image segmentation. To study a specific object in an image, its boundary can be highlighted by an image segmentation procedure. The objective of the image segmentation is to simplify the representation of pictures into meaningful information by partitioning into image regions. Image segmentation is a technique to locate certain objects or boundaries within an image. There are many algorithms and techniques have been developed to solve image segmentation problems, the research topics in this book such as level set, active contour, AR time series image modeling, Support Vector Machines, Pixon based image segmentations, region similarity metric based technique, statistical ANN and JSEG algorithm were written in details. This book brings together many different aspects of the current research on several fields associated to digital image segmentation. Four parts allowed gathering the 27 chapters around the following topics: Survey of Image Segmentation Algorithms, Image Segmentation methods, Image Segmentation Applications and Hardware Implementation. The readers will find the contents in this book enjoyable and get many helpful ideas and overviews on their own study.

InTech Europe
University Campus STeP Ri
Slavka Krautzeka 83/A
51000 Rijeka, Croatia
Phone: +385 (51) 770 447
Fax: +385 (51) 686 166
www.intechopen.com

InTech China
Unit 405, Office Block, Hotel Equatorial Shanghai
No.65, Yan An Road (West), Shanghai, 200040, China
中国上海市延安西路65号上海国际贵都大饭店办公楼405单元
Phone: +86-21-62489820
Fax: +86-21-62489821

IntechOpen